Journal of Renewable Energies

Revue des Energies Renouvelables

journal home page : https://revue.cder.dz/index.php/rer

Fuzzy Logic PI controller based Direct Torque control of a Self-Excited Induction Generator through a three-level Rectifier

Kahina Berabez [a,]*, Farid Hamoudi [b], Kassa Idjdarene [a] Ismail Hacini [a]

[a] *Laboratoire de Technologie Industrielle et de l'Information, Faculté de Technologie, Université de Bejaia. 06000 Bejaia, Algeria*

[b] *2Laboratoire de Maitrise des Energies Renouvelables, Faculté de Technologie, Université de Bejaia. 06000 Bejaia, Algeria.*

* *Corresponding author, E-mail address: kahina.berabez@univ-bejaia.dz*

Tel.: + ___ __________

Abstract

The main goal of this work is to control the terminal voltage of a Self-excitation induction generator (SEIG) that supplies autonomous load and is driven by a variable speed wind turbine. More advanced strategies of control have been suggested and applied these through a two-level converter. However, in this paper, we propose to study a modified DTC approach which based on the use of three-level converter (NPC structure) and instead of the traditional PI controller, we use a PI fuzzy controller to reduce torque and flux ripples, the induction generator's stator flux and electromagnetic torque are controlled using voltage space vector selection. The proposed control strategy has to maintain constant DC bus voltage regardless of load or wind speed variations. Finally, it should be noted that this control accounts for the induction generator's magnetic saturation phenomenon.

Keywords: Induction generator, DTC control, 3L_NPC converter, Fuzzy logic controller, autonomous.

1. Introduction

Over the years, standalone operation of wind turbine-based squirrel cage induction generator is commonly employed in isolated or remote areas [1] of due to its advantages such as: high performance, the ability of operating under variable wind speed, robustness and low cost [1], [2]. Furthermore, Self-excitation for these machines can be achieved by connecting capacitance bank connected at the stator terminals or by employing an inverter/rectifier system with a single DC capacitor on the DC link side [3], [4]. this needs high-performance control. For ensure a wished regulation, several techniques of control have been reported and established in literature such as: the field-oriented control techniques and the direct torque control these techniques are the most commonly utilized strategies. Unlike a flux-oriented control the, Direct torque control (DTC) regulates the electromagnetic torque and the stator flux of the electrical machine directly and independently [5] and it is now one of the most widely utilized control approaches for overcoming the complexity and the problems of conventional controls and to enhance of performance of the induction generator [6]. However, despite the outstanding performance of classical DTC, it has followed some drawbacks like. uncontrollable switching frequency which causes commutation losses and current distortions, which can affect output power quality [7], [8]. for this purpose, studies have been conducted to address the aforementioned problems. The authors in [2] are used the Space Vector Modulation (DTC_SVM) technique. Where, the switching table is replaced by the SVM algorithm in this method, and the hysteresis comparators are replaced by PI controllers. Another technique based to use of 12 sectors instead of six to reduce flux undulations is proposed by [9], [10]. in [9], [11] the authors have used of fuzzy logic regulators instead hysteresis regulators. Even with the remarkable performance in these approaches which are proved their good performance in the case of controlling. However, in the conventional DTC method through a two-level converter, important ripples in torque and flux are caused by a limited number of voltage vectors in the two-level [12], the waveform of voltages and currents have a high harmonic distortion in addition, the maximum voltage that semiconductor switching devices can support is the magnitude of the DC bus voltage [13]. Moreover, for stand-alone systems that requires the use of high-power machines, such converter is more than advantageous. So, many of these constraints and limitations can be significantly reduced and resolved by using the new multilevel converter topologies. This is one of the motivations of the present study, in which a multilevel converter (inverter/rectifier) is proposed to the terminal voltage control of a self-exited induction generator with direct torque control technique based on the three-level neutral point clamped (3L-NPC). The DC voltage is kept constant, by regulating the voltage at the rectifier output with fuzzy logic control approaches This control technique does not require a precise mathematical model because it is based solely on linguistic rules. It is also nonlinear and adaptive in nature that gives it robust performance under parameter variation. this control accounts for the magnetic phenomenon of the (SEIG) via a magnetization inductance L_m who will be presented by the following by a polynomial approximation as a function of the magnetization current i_m. The performances of the proposed control strategy are verified and confirmed through simulation tests under MATLAB®-SIMULINK.

2. Studied System and Model

The system studied for standalone generating with SEIG, wind turbine, a Three-level neutral point clamped rectifier/inverter (3L_NPC), an autonomous load, along with DC side along with the proposed control strategy are shown in Fig. 4.

2.1 Induction machine model

The linear model of squirrel-cage asynchronous machine is describing by equations electrical in the two-phase (α-β) reference by following while the saturation effect is considered in a global manner through the only first harmonic:

$$\begin{bmatrix} V_{s\alpha} \\ V_{s\beta} \\ 0 \\ 0 \end{bmatrix} = \begin{bmatrix} R_s & 0 & 0 & 0 \\ 0 & R_s & 0 & 0 \\ -R_r & \omega_r .l_r & R_r & -\omega_r .(l_r + L_m) \\ -\omega_r .l_r & -R_r & \omega_r .(l_r + L_m) & R_r \end{bmatrix} . \begin{bmatrix} i_{s\alpha} \\ i_{s\beta} \\ i_{m\alpha} \\ i_{m\beta} \end{bmatrix} +$$

$$\begin{bmatrix} l_s & 0 & L_m + L_m' .\frac{i_{m\alpha}^2}{|i_m|} & L_m' .\frac{i_{m\alpha}.i_{m\beta}}{|i_m|} \\ 0 & l_s & L_m' .\frac{i_{m\alpha}.i_{m\beta}}{|i_m|} & L_m + L_m' .\frac{i_{m\beta}^2}{|i_m|} \\ -l_r & 0 & l_r + L_m + L_m' .\frac{i_{m\alpha}^2}{|i_m|} & L_m' .\frac{i_{m\alpha}.i_{m\beta}}{|i_m|} \\ 0 & -l_r & L_m' .\frac{i_{m\alpha}.i_{m\beta}}{|i_m|} & l_r + L_m + L_m' .\frac{i_{m\beta}^2}{|i_m|} \end{bmatrix} . \begin{bmatrix} \frac{di_{s\alpha}}{dt} \\ \frac{di_{s\alpha}}{dt} \\ \frac{di_{m\alpha}}{dt} \\ \frac{di_{m\beta}}{dt} \end{bmatrix} \quad (1)$$

Where: Rs, Rr, are the stator and rotor phase resistances, Lr is the self-inductances respectively, L_m is the magnetizing inductance. is the mutual inductance, Ω the speed. vsα, vsβ, isα and isβ: are the (α-β) axis components of the stator voltages and currents respectively.

$i_{m\alpha}$ and $i_{m\beta}$ are the magnetizing currents, along the α and β axis, given by:

$$\begin{cases} i_{m\alpha} = i_{s\alpha} + i_{r\alpha} \\ i_{m\beta} = i_{s\beta} + i_{r\beta} \end{cases} \quad (2)$$

$$i_m = \sqrt{{i_{m\alpha}}^2 + {i_{m\beta}}^2} \tag{3}$$

The magnetizing inductance L_m with respects to im is well detailed and presented in reference [4].

2.2 Three-level NPC converter and DC link mode

The Three-level neutral point clamped inverter (NPC) is shown in Fig.1 It built-up of twelve fully-controlled switches, each one with its freewheeling diode and two power diodes located in each phase leg that allow the connection of the phase output to the midpoint of the DC bus that at consists of two capacitors in series, the three levels of output voltages generated -Vdc/2, 0 and -Vdc are obtained by combination of the 12 switches. There are 27 different three-phase voltage outputs determined by 27 different switch combinations [12] [13].

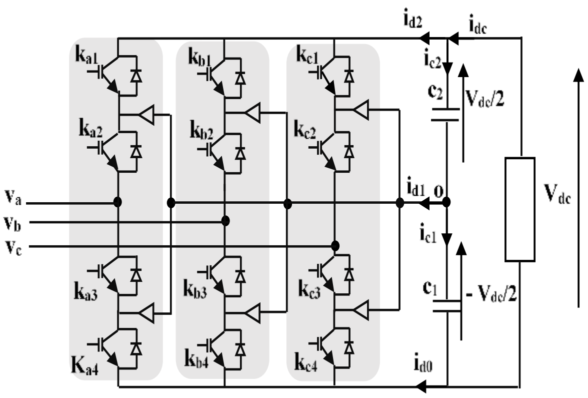

Fig.1. Schematic of a three-level NPC inverter

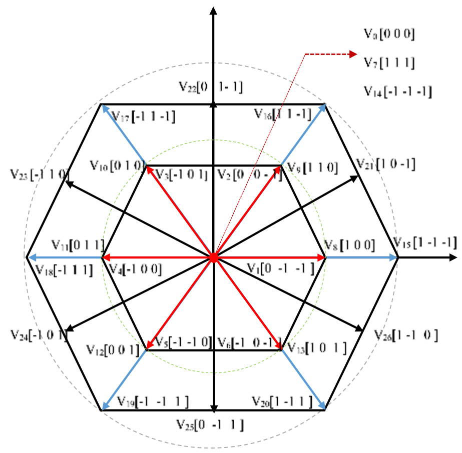

Fig.2. Space voltage vector [15].

a connection function is defined for each state h of the arm x is given in following equation [12] : $F_x^2 = S_{x1} S_{x2}$ $\quad F_x^1 = S_{x1} \overline{S_{x2}}$ $\quad F_x^0 = \overline{S_{x1}}\,\overline{S_{x2}}$ (4)

The following equation expresses the three voltage levels based on the connection functions:

$$v_{xo} = V_{dc}(F_x^2 - F_x^0) \tag{5}$$

The leg voltages can then be written as[16]:

$$\begin{bmatrix} v_a \\ v_b \\ v_c \end{bmatrix} = \frac{V_{dc}}{3} \begin{bmatrix} 2 & -1 & -1 \\ -1 & 2 & -1 \\ -1 & -1 & 2 \end{bmatrix} \begin{bmatrix} F_a^2 - F_a^0 \\ F_b^2 - F_b^0 \\ F_c^2 - F_c^0 \end{bmatrix} \tag{6}$$

The i_{dc} current is given by the equation: $i_{dc} = i_b - i_R - i_c$ (7)

With: $i_c = C\frac{dV_{dc}}{dt}$ (8)

The dc voltage can be represented by the following equation:

$$V_{dc} = -\int \frac{1}{C}\left(i_{dc} + V_{dc}\left(\frac{1}{R} + \frac{1}{r_b}\right) - \frac{V_0}{r_b}\right) \quad (9)$$

Where V_0: the initial voltage across the capacitor (i.e., the battery voltage). When the diode is blocked, the DC voltage becomes $V_{dc} \geq V_0$.

Then, the dc voltage become: $V_{dc} = -\int \frac{1}{C}\left(i_{dc} + \frac{V_{dc}}{R}\right)$ (10)

3. Control Strategy

3.1 Direct torque control strategy

Direct torque control (DTC) aims to directly regulate the torque of the machine. The system's performance can be improved by increasing the level degree of the inverters used, allowing for a wider range of voltage vector selection based on the level of variation in the torque and flux error values. The controlled variables are the stator flux and the electromagnetic torque, two hysteresis comparators of (5 & 3 level) are using for controlled the (Tem and flux) respectively. The proposed control strategy has to keep the DC bus voltage constant, regardless of the variations the load and wind speed, which achieved by controlling the electromagnetic torque depending on the speed. The space of evolution of the flux is divided into twelve sectors (1…12) of 30° each. this choice is detected for the sake of more rigorous control and such that:

$$\frac{-\pi}{12} + (i-1)\frac{\pi}{6} \leq S(i) \langle \frac{\pi}{12} + (i-1)\frac{\pi}{6} \quad (11)$$

The converter switching states can be selected from a switching table (see Table 1) [7] [14] This last determines the set of 27 optimal voltage vectors of converter to be applied at each switching instant.

The vector model of the SEIG can emphasize the dynamic control conditions on the electromagnetic torque of the induction machine. For that one, we present in the spatial vector the machine's electrical equations [6]

$$\begin{aligned} \overline{V_s} &= R_s \overline{I_s} + \frac{d\overline{\Phi_s}}{dt} \\ 0 &= R_r \overline{I_r} + \frac{d\overline{\Phi_r}}{dt} - j\omega\overline{\Phi_r} \end{aligned} \quad (12)$$

The voltage vector Vs is delivered by a 3L_NPC converter and we can be written based on the connection functions in the form [7]:

$$\overline{V_s} = \sqrt{\frac{3}{2}} V_{dc} (S_a + S_b{}^{j\frac{2\pi}{3}} + S_c{}^{j\frac{4\pi}{3}}) \tag{13}$$

It is worthy noted that the stationary reference frame has using for estimating the stator flux and Tem from the expressions of stator current and stator voltage, which are given by the following equations [6]:

$$\begin{cases} i_{s\alpha} = \sqrt{\frac{3}{2}} i_{sa} \\ i_{s\beta} = \sqrt{\frac{1}{2}} (i_{sb} - i_{sc}) \end{cases} \tag{14}$$

$$\begin{cases} V_{s\alpha} = \sqrt{\frac{3}{2}} V_{dc} (S_a - \frac{1}{2}(S_b - S_c)) \\ V_{s\beta} = \sqrt{\frac{1}{2}} V_{dc} (S_b - S_c) \end{cases} \tag{15}$$

The magnitude of the stator flux is given by:

$$\Phi_s = \sqrt{\Phi_{s\alpha}^2 + \Phi_{s\beta}^2} \tag{16}$$

Where:

$$\begin{cases} \Phi_{s\alpha} = \int_0^t (V_{s\alpha} - R_s i_{s\alpha}) dt \\ \Phi_{s\beta} = \int_0^t (V_{s\beta} - R_s i_{s\beta}) dt \end{cases} \tag{17}$$

3.2 Fuzzy logic control

Fuzzy logic controllers use reasoning in the same way that humans do. As a result, the controller rules include expert knowledge of the system. The fuzzy modelling process requires four steps: (i)The Fuzzy modelling approach begins with defining and building the control inputs vector (fuzzification), (ii) Construct the function intervals (iii) Define the fuzzy output variable sets finally, we define the fuzzy rules (defuzzification). The fuzzy(PI) controller proposed in this study has two inputs, error E and change of error DE and one output, we use seven fuzzy sets to convert it into linguistic variable Positive Big (PB), Positive Medium (PM), Positive Small

(PS), Zero (ZE), Negative Small (NS), Negative Medium (NM), Negative Big (NB). the proposed Memberships function form for both input and output are shown in the Fig.4 and table 2 [15].

Table 1. DTC switching table 27 vectors.

Δ_φ	Δ_{Tem}	Sectors S_i											
		S_1	S_2	S_3	S_4	S_5	S_6	S_7	S_8	S_9	S_{10}	S_{11}	S_{12}
	+2	V_{21}	V_{16}	V_{22}	V_{17}	V_{23}	V_{18}	V_{24}	V_{19}	V_{25}	V_{20}	V_{26}	V_{15}
-1	+1	V_{21}	V_{02}	V_{22}	V_{03}	V_{23}	V_{04}	V_{24}	V_{05}	V_{25}	V_{06}	V_{26}	V_{01}
	0	V_{00}	V_{07}	V_{14}	V_{00}	V_{07}	V_{14}	V_{00}	V_{07}	V_{14}	V_{00}	V_{07}	V_{14}
	-1	V_{26}	V_{01}	V_{21}	V_{02}	V_{22}	V_{03}	V_{23}	V_{04}	V_{24}	V_{05}	V_{25}	V_{06}
	-2	V_{26}	V_{15}	V_{21}	V_{16}	V_{22}	V_{17}	V_{23}	V_{18}	V_{24}	V_{19}	V_{25}	V_{20}
	+2	V_{22}	V_{17}	V_{23}	V_{18}	V_{24}	V_{19}	V_{25}	V_{20}	V_{26}	V_{15}	V_{21}	V_{16}
	+1	V_{22}	V_{03}	V_{23}	V_{04}	V_{24}	V_{05}	V_{25}	V_{06}	V_{26}	V_{01}	V_{21}	V_{02}
0	0	V_{00}	V_{07}	V_{14}	V_{00}	V_{07}	V_{14}	V_{00}	V_{07}	V_{14}	V_{00}	V_{07}	V_{14}
	-1	V_{25}	V_{06}	V_{26}	V_{01}	V_{21}	V_{02}	V_{22}	V_{03}	V_{23}	V_{04}	V_{24}	V_{05}
	-2	V_{25}	V_{20}	V_{26}	V_{15}	V_{21}	V_{16}	V_{22}	V_{17}	V_{23}	V_{18}	V_{24}	V_{19}
	+2	V_{17}	V_{23}	V_{18}	V_{24}	V_{19}	V_{25}	V_{20}	V_{26}	V_{15}	V_{21}	V_{16}	V_{22}
	+1	V_{03}	V_{23}	V_{04}	V_{24}	V_{05}	V_{25}	V_{06}	V_{26}	V_{01}	V_{21}	V_{02}	V_{22}
1	0	V_{00}	V_{07}	V_{14}	V_{00}	V_{07}	V_{14}	V_{00}	V_{07}	V_{14}	V_{00}	V_{07}	V_{14}
	-1	V_{05}	V_{25}	V_{06}	V_{26}	V_{01}	V_{21}	V_{02}	V_{22}	V_{03}	V_{23}	V_{04}	V_{24}
	-2	V_{19}	V_{25}	V_{20}	V_{26}	V_{15}	V_{21}	V_{16}	V_{22}	V_{17}	V_{21}	V_{18}	V_{24}

Table 2. Fuzzy-PI rule

E/dE	NB	NM	NS	ZE	PS	PM	PB
NB	NB	NB	NB	NB	NM	NS	NS
NM	NB	NB	NB	NM	NS	NS	NS
NS	NB	NB	NM	NS	PS	PM	PB
ZE	NS	NS	NS	ZE	PS	PS	PS
PS	PS	PS	PS	PS	PM	PM	PB
PM	PS	PS	PS	PM	PB	PB	PB
PB	PS	PS	PM	PB	PB	PB	PB

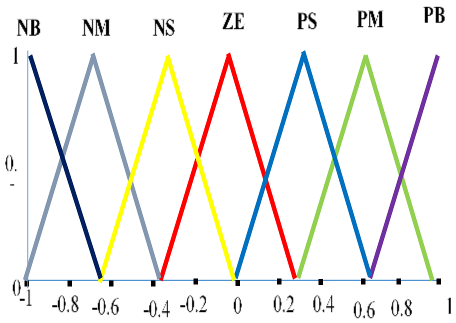

Fig.3. Input output membership function

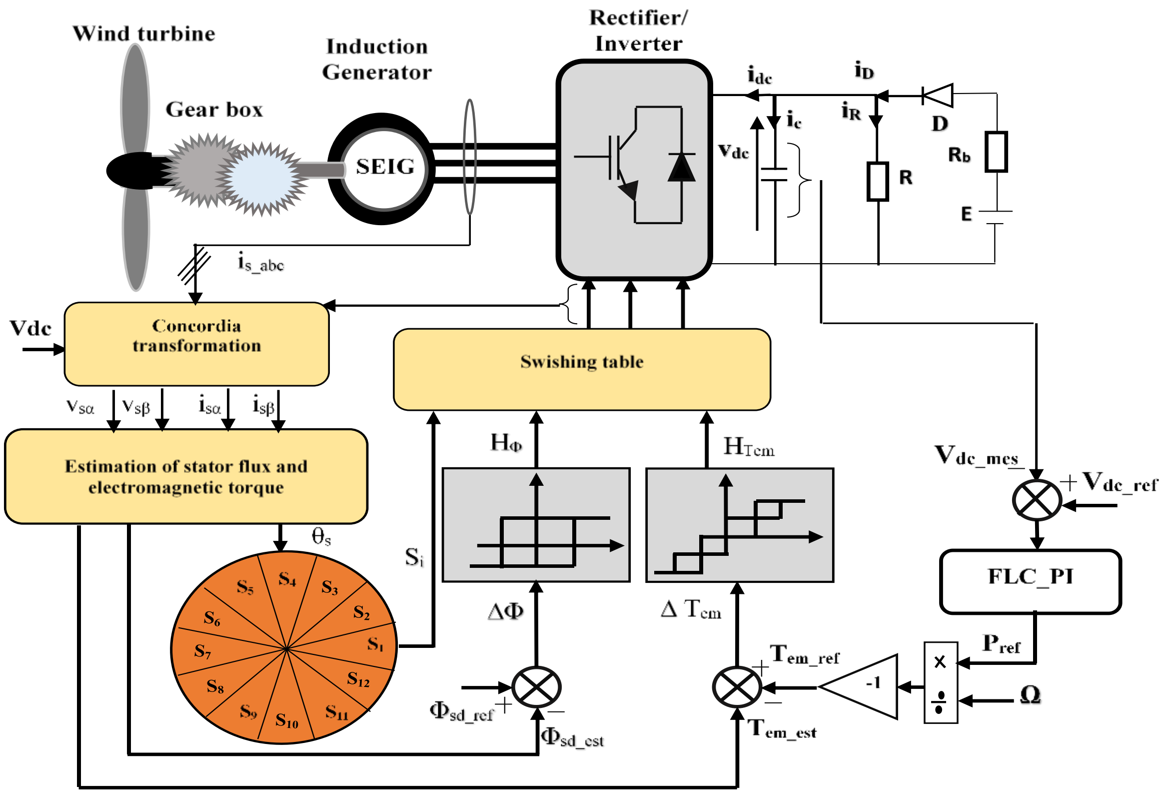

Fig.4. System and DTC strategy scheme

4. Simulation Result

To illustrate the behaviour of the DTC control structure using fuzzy logic regulator with a 3L_NPC converter, applied a SEIG tests simulations tests carried out under the MATLAB®-SIMULINK environment. In this study, the SEIG is driven at a synchronous speed in the start-up, then is applied as indicated in the figure 5. this last show that there are three levels of speed, the synchronism speed, i.e., 750 rpm. At t = 2s, we applied a decrease of 10% of synchronism speed then an increase also of 10% at t=6s. Finally, at t= 8s, the speed is recovered to its synchronous value and remains constant. In the second case, after recovering the synchronous speed, a load change is applied at t=10s by increasing the DC load resistance from 70 to 90Ω, (50%) during 2 seconds. Then, the resistance is gradually decreased as shown in Fig. 6. The DC voltage reference is set at 465V, while the flux reference is set to 0.7Wb. The Fig.7 shows that the DC bus voltage is well regulated and is sensitive to speed and load variations. However, these disturbances are quickly rejected. Fig.8 depicts the evolution of electromagnetic torque according to the speed and load variations. These variations can be seen to have an effect on the torque Tem. The estimated flux tracks finely its reference without any overshoot and it is disturbed neither by the speed variations nor by the load change Fig.9.. The evolutions of the flux ($\varphi s\alpha$, $\varphi s\beta$) take sinusoidal waveforms as represented in Fig.10. In Fig.11is represented the voltage vector trajectory in (α, β). The evolution of the flux Φsβ with respect to Φsα given in Fig .11 is a perfectly circular Finally, in Fig 12, one can see that the shape of the stator current is sinusoidal. Furthermore, the stator currents are harmonics free, as illustrated by the spectrum in Fig. 13, with THD of 0.36%.

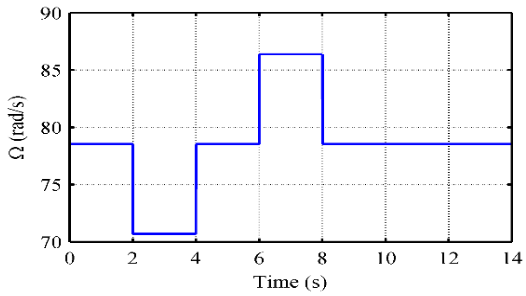

Fig.5 Profile of the driving speed

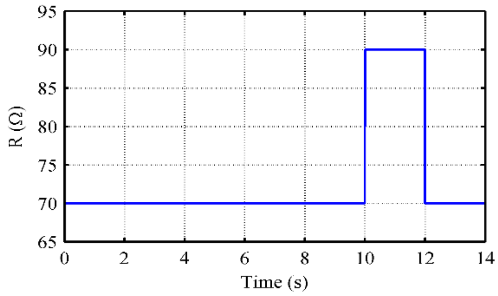

Fig.6 Profile of the load variation

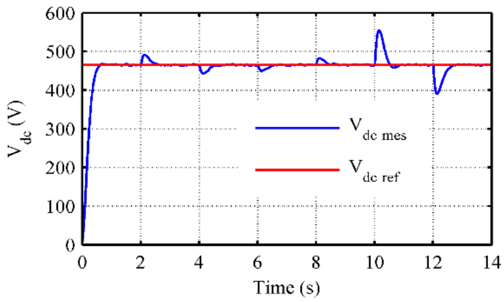

Fig.7 The DC voltage

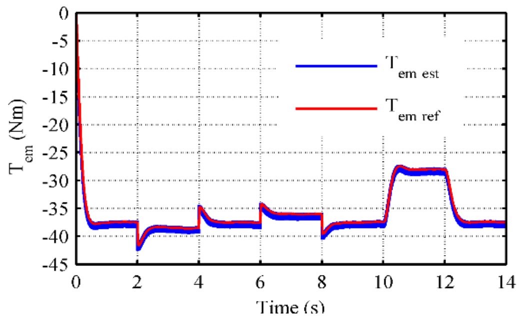

Fig .8 Electromagnetic torque evolution

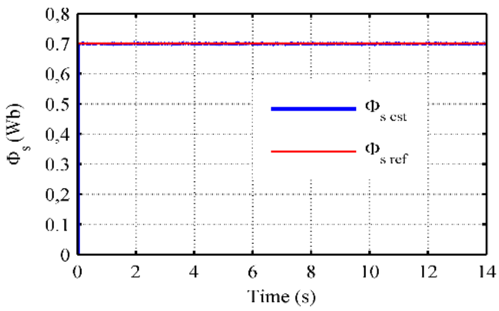

Fig .9 The stator flux magnitude

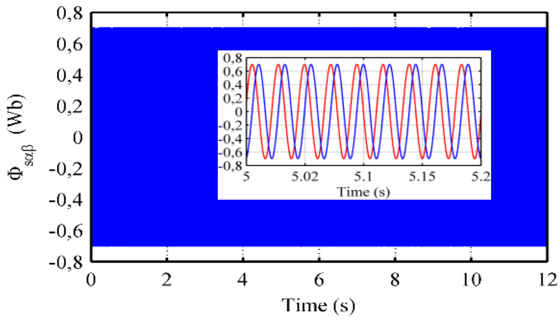

Fig .10 The flux (φsα, φsβ)

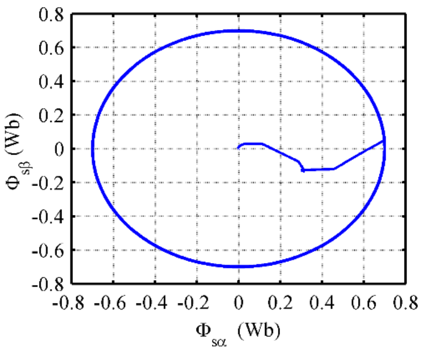

Fig.11 stator flux trajectory

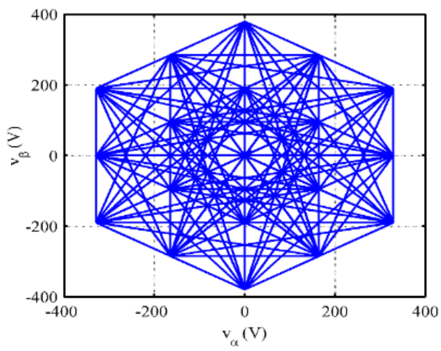

Fig.12 The trajectory of the voltage vectors

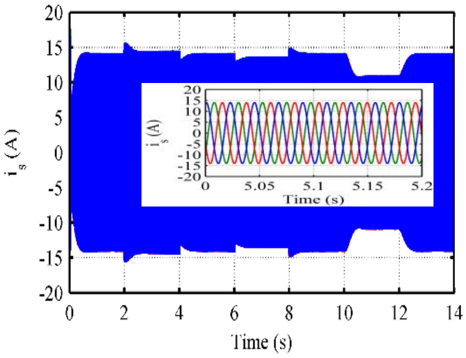

Fig .13. The stator current

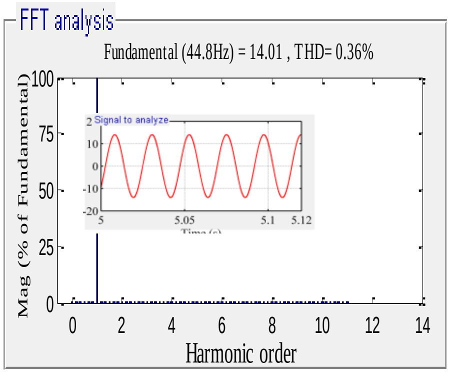

Fig.14. The spectral analysis (THD)

5. Conclusion

The study presented in this paper aims an enhancement the performance of the SEIG in an autonomous variable speed wind system using direct torque control based of 3L_NPC structure three levels converter and a fuzzy PI controller. The analytical diphase model of the (SEIG) based on the application of the Concordia transform is introduced while taking into account the saturation phenomenon. The simulation results confirm that this control strategy showed a significant reduction in flux and torque ripples. lowering of the THD of stator currents. Therefore, the studied system demonstrates the effectiveness of the proposed control such as: The objective of maintaining voltage in dc-link is carried out effectively and a good regulation of the flux and electromagnetic torque according to a variation of the driving speed and load.

6. Acknowledgements

The project presented in this paper is supported by the Laboratory of Industrial Technology and the Information (LTII) of Bejaia University under the patronage of the General Directorate of Scientific Research and Technological Development (DGRSDT), Algeria.

7. References

[1] Laddi, T., Taib, N., &Aouzellag, D. "A Proposed Strategy for Power Management of a Standalone Wind Energy Conversion System with Storage Battery". Periodica Polytechnica Electrical Engineering and Computer Science, 64(3), 229-238, 2020. doi: 10.3311/PPee.15094.

[2] Issad. I., Idjdarene.K and Lalouni.S. "direct torque control using space vector modulation of wind pumping system with storage". Revue Roumaine des Sciences Techniques-Serie Electrotechnique et Energetique Vol. 63, 4, pp. 397–402, Bucarest, 2018.

[3] Seyoum, D., M. F. Rahman and C. Grantham. "Inverter supplied voltage control system for an isolated induction generator driven by a wind turbine". in 38th IAS Annual Meeting on

Conference Record of the Industry Applications Conference, 2003., Salt Lake City, UT, USA, 2003, vol. 1, pp. 568–575, ISBN 978-0-7803-7883-40. doi:10.1109/IAS.2003.1257557

[4] Aberbour. A., K. Idjdarene and Z. Boudries. " Adaptable sliding mode control for wind energy application". Revue Roumaine des Sciences Techniques-Serie Electrotechnique et Energetique. Vol. 61, 3, pp. 258–262, Bucarest, 2016.

[5] Choi, Y. S., Choi, H. H., & Jung, J. W. "Feedback linearization direct torque control with reduced torque and flux ripples for IPMSM drives". IEEE Transactions on Power Electronics, 31(5), 2015: 3728-3737.doi: 10.1109/TPEL.2015.2460249.

[6] Idjdarene, K., Rekioua, D., Rekioua, T., & Tounzi, A. "Direct torque control strategy for a variable speed wind energy conversion system associated to a flywheel energy storage system." 2009 Second International Conference on Developments in eSystems Engineering. IEEE, 2009. doi: 10.1109/DeSE.2009.47.

[7] El Ouanjli, Najib, & al. "Direct torque control of doubly fed induction motor using three-level NPC inverter." Protection and Control of Modern Power Systems 4.1 (2019): 1-9. doi: /10.1186/s41601-019-0131-7.

[8] Mesloub, Hayette, & al. "Comparative study of conventional DTC and DTC_SVM based control of PMSM motor—Simulation and experimental results." Mathematics and Computers in Simulation 167 (2020): 296-307.doi: 10.1016/j.matcom.2018.06.003.

[9] Belaid, S. L. "Improved IM DTC by using a Fuzzy Switching Table in PV Applications". Elektrotehniski Vestnik, 88(1/2), 26-32.

[10] Sahri, Younes, & al. "Advanced Fuzzy 12 DTC Control of Doubly Fed Induction Generator for Optimal Power Extraction in Wind Turbine System under Random Wind Conditions." Sustainability 13.21 (2021): 11593.doi: doi.org/10.3390/su132111593.

[11] Dagang, C. T. S., Kenne, G., & Muluh, F. A. "Fuzzy logic direct torque/power control for a self-excited induction generator driven by a variable wind speed turbine." International Journal of Dynamics and Control 9.3 (2021): 1210-1222.doi: 10.1007/s40435-020-00709-9.

[12] Aissa, O., Moulahoum, S., Kabache, N., & Houassine, H «Improvement of DTC of induction motors by using a three-level inverter and fuzzy speed controller." 22nd Mediterranean Conference on Control and Automation. IEEE, 2014.doi: 10.1109/MED.2014.6961329.

[13] Benyoussef, E., & Barkat, S. "Three-level direct torque control based on balancing strategy of five-phase induction machine": n/a. revue roumaine des sciences techniques—série électrotechnique et énergétique, 67(2),2022: 93-98.

[14] Messaïf, I., Berkouk, E. M., & Saadia, N. "Ripple reduction in DTC drives by using a three-level NPC VSI". In 2007 14th IEEE International Conference on Electronics, Circuits and Systems. 2007, December, (pp. 1179-1182). IEEE. doi: 10.1109/ICECS.2007.4511206.

[15] Meddouri, S., Idjdarene, K., & Aberbour, A. "Fuzzy vector control of isolated induction generator taking the saturation effect into account." 2014 International Conference on Electrical Sciences and Technologies in Maghreb (CISTEM). IEEE, 2014.doi: 10.1109/CISTEM.2014.7077056.